Available online at www.sciencedirect.com
SCIENCE DIRECT®
Mutation Research 581 (2005) 141–152
Genetic Toxicology and Environmental Mutagenesis
www.elsevier.com/locate/gentox
Community address: www.elsevier.com/locate/mutres

Combined effects of gamma radiation and arsenite on the proteome of human TK6 lymphoblastoid cells

Soile Tapio[a,*], Joana Danescu-Mayer[a], Monika Asmuss[a], Anton Posch[b], Maria Gomolka[a,1], Sabine Hornhardt[a,1]

[a] *Federal Office for Radiation Protection, Department of Radiation Protection and Health, Ingolstaedter Landstrasse 1, 85764 Neuherberg, Germany*
[b] *Tecan Munich GmbH, Feldkirchner Strasse 12a, 85551 Kirchheim, Germany*

Received 26 August 2004; received in revised form 18 November 2004; accepted 29 November 2004
Available online 18 January 2005

Abstract

Arsenic present in drinking water and mining environments in some areas has been associated with an increased rate of skin and internal cancers. Contrary to the epidemiological evidence in humans, arsenic does not induce cancer in animal models, but is able to enhance the mutagenicity of other agents. In order to achieve a better understanding of the interaction between arsenic and ionising radiation, an investigation was conducted to detect differences at the proteome level of human TK6 lymphoblastoid cells exposed to these agents. Cells were exposed to either a single dose of 1-Gy ^{137}Cs-γ-rays or to 1 μM arsenite (As(III)) or to both agents in combination. Two-dimensional (2D) electrophoresis and matrix-assisted laser desorption/ionisation-time of flight (MALDI-TOF) were employed for the screening and identification of proteins, respectively. It proved possible to identify seven proteins with significantly affected abundance, three of which showed increased levels and the remaining four showed decreased levels under at least one of the exposure conditions. Following arsenite treatment or irradiation, a significant increase compared with that of the control was observed for glutathione (GSH) transferase omega 1 and proteasome subunit beta type 4 precursor. The combined exposure did not result in an induction of the enzymes. The expression of electron-transfer flavoprotein subunit alpha was found to be enhanced under all three-exposure conditions. Ubiquinol-cytochrome *C* reductase complex core protein I, adenine phosphoribosyl transferase and endoplasmic reticulum protein hERp29 showed decreased levels after irradiation or arsenite treatment, but not after the combined exposure. The level of serine/threonine protein phosphatase 1 alpha decreased with all treatments. The main conclusions are that both arsenite and γ-radiation influence the levels of several proteins involved in major metabolic and regulatory pathways, either directly or by triggering the defence mechanisms of the cell. The combined effect of both exposures on the level of some essential proteins such as glutathione transferase, proteasome or serine/threonine phosphatase may contribute to the co-carcinogenic effect of arsenic.

Keywords: Arsenite; Gamma radiation; Proteomics; Carcinogenesis; Human TK6 lymphoblastoid cells

* Corresponding author. Tel.: +49 1888 333 2258; fax: +49 1888 333 2205.
E-mail address: stapio@bfs.de (S. Tapio).
[1] The authors contributed equally to the investigation.

1383-5718/$ – see front matter © 2004 Elsevier B.V. All rights reserved.
doi:10.1016/j.mrgentox.2004.11.016

1. Introduction

Arsenic is a semi-metal present in the upper crust of the earth. The form of arsenic in the environment that is most likely to be mutagenic is arsenite (As(III)) [1]. In its soluble form, it is a contaminant in freshwater, salt water and air. Arsenite in drinking water is associated with the development of cancer of the skin [2], lung, kidney [3], liver and bladder [4]. Acidic mining environments are of particular concern with regard to arsenic pollution: the inhalation of arsenic, combined with exposure to ionising radiation (IR) is known to increase the rate of human lung cancer [5–7].

In spite of accruing information about the cellular targets of arsenite and the counterparts in its mode of action, its specific mechanism is still unknown, possibly because it shows little or no mutagenetic potential in bacteria or in animal models [8]. However, arsenite in combination with other DNA-damaging agents such as UV light [9], alkylating agents [10] or DNA-cross-linking agents [11] enhances their cyto- and genotoxic effects already at low, non-toxic concentrations. Since arsenite reacts with vicinal dithiol groups in proteins [12], inhibits the nucleotide excision repair [13] and forms DNA-protein cross-links [14], it was hypothesised to be co-carcinogenic by inhibiting enzymes involved in DNA repair. However, no arsenite-sensitive DNA repair enzymes have been identified until now, with the exception of poly(ADP-ribose)polymerase (PARP) [15].

Early studies highlighted the interplay between arsenite and mitochondrial energy-linked functions such as inhibition of oxygen utilisation [16], pyruvate dehydrogenase activity [17], gluconeogenesis and the citric acid cycle [18]. Nowadays, it is known that the electron-transport chain of mitochondria consumes more than 90% of the oxygen taken up by the cell and is, even during normal physiological conditions, the major source of reactive oxygen species (ROS) [19], which damage various biomolecules including DNA. Arsenite increases the intracellular level of ROS [20] presumably leading to the induction of DNA breaks [21] as well as different cellular responses such as the increase of intracellular glutathione (GSH) content [22], disturbed redox regulation [23], stress response [24,25] and apoptosis [26,27].

Even though epidemiological studies have underlined the co-carcinogenic role of arsenic compounds together with ionising radiation in humans, there are only a few studies available dealing with the interaction of these noxious agents at the biological level. The existing data are based on very high-radiation doses [28] or concentrate on a certain cellular response [29]. The aim of the present work was to screen for all candidate pathways involved in the outcome of the combined exposure. Recent developments in the cellular proteome analysis have made possible the characterisation of differences in protein expression levels and the identification of proteins repressed or induced [30] when cells are exposed to multiple toxicants.

As a model system the changes in the proteome of the human lymphoblastoid cell line TK6, treated separately or simultaneously with arsenite and ^{137}Cs-γ-rays, were investigated. Two-dimensional (2D) gel electrophoresis and matrix-assisted laser desorption/ionisation-time of flight (MALDI-TOF) mass spectrometry were applied for screening and identification of the protein spots, respectively. In order to mimic the in vivo situation, both exposures were kept relatively low. Arsenite was used at the non-toxic concentration of 1 μM [31], well below the concentrations found in the drinking water of arsenic-rich areas [32], and a radiation dose of 1-Gy ^{137}Cs-γ-rays was applied. From previous investigations, it was clear that DNA repair after irradiation damage, measured with the alkaline comet assay in TK6 cells was rapid, most of the damage being repaired within 15 min [33]. Therefore, it was necessary to measure the immediate response to irradiation in the nuclear fraction of cells that were also exposed for a longer time (22 h) to arsenite.

2. Materials and methods

2.1. Cell culture, exposure conditions and protein extraction

TK6 cells, a human lymphoblastoid cell line, were grown as a suspension culture in RPMI 1640 medium supplemented with 20% inactivated fetal calf serum (FCS), 1% non-essential amino acids and 1% sodium pyruvate [113-24-6] (all from Biochrom) at 37 °C in an atmosphere of 5% CO_2.

Logarithmically growing TK6 cells were portioned into four equal samples. Two samples were treated for 22 h with the final concentration of 1 μM sodium

arsenite ($AsNaO_2$) [7784-46-5] (Fluka); the stock solution (1 mM $AsNaO_2$ in fresh medium) was added slowly with light rotational shaking to avoid high local concentrations of As(III). A similar amount of fresh medium was added to the two other samples.

Twenty-two hours after adding the arsenite solution or the medium only, one As(III)-treated sample and one sample without As(III) treatment were irradiated in culture flasks with a dose of 1-Gy ^{137}Cs-γ-rays (69 cGy/min; HWM-2000, Markdorf), giving the following combination of samples: one untreated control sample, one sample irradiated with γ-rays, one sample treated with As(III) and one sample treated with As(III) and irradiated.

After irradiation, the cells were further incubated for 15 min at 37 °C, pelleted at a concentration of 1×10^6 cells/ml by centrifugation ($200 \times g$, 4 °C, 10 min), washed with cold Ca(II)- and Mg(II)-free phosphate-buffered saline (PBS) (Biochrom) pH 7.5, and resuspended in lysis buffer containing 6 M urea [57-13-6] (Roth), 2 M thiourea [62-56-6] (Fluka), 2% CHAPS [75621-03-3] (Merck), 1% dithiothreitol (DTT) [3483-12-3], sodium dodecyl sulfate (SDS) [151-21-3] (Bio-Rad), 0.5% Pharmalyte 5-8 (Bio-Rad) and 5 mM Pefabloc (Merck) [34]. The lysis of the cell membrane occurring at room temperature (RT) with shaking was monitored microscopically by adding 0.025% Trypan blue [72-57-1] (Seromed) in PBS to samples of the cell extract (27:1). The nuclear fraction was separated from the cytosolic fraction by centrifugation ($3000 \times g$, 15 °C, 15 min), suspended in lysis buffer and lysed further as described above. After the lysis of the nuclear membrane, observed microscopically with SYPRO Green (Sigma), the enriched nuclear fraction and the cytosolic fraction were centrifuged at $40{,}000 \times g$ for 1 h at 15 °C. The enriched nuclear fraction was further purified using Plus One Clean Up Kit (Amersham Biosciences) according to the manufacturer's instructions and, after defining the protein content of the supernatant by Ettan 2D-Quant Kit (Amersham Biosciences) used for further analysis.

2.2. 2D-electrophoresis (2D-E)

For isoelectric focusing (IEF), samples containing 60 μg protein for analytical and 300 μg protein for preparative purposes, respectively, were suspended in rehydration buffer (6 M urea, 2 M thiourea, 2% CHAPS, 0.4% DTT, 0.5% Pharmalyte 5-8 and 5 mM Pefabloc) to reach a final volume of 300 μl. The sample loading was done by the active in-gel-rehydration for the analytical samples (50 V, 12 h) or by the passive in-gel-rehydration overnight for the preparative samples on 17-cm Ready Strip IPG-Strips, linear pH 5–8, in the Protean IEF cell system (Bio-Rad). The entire set-up was covered with low-viscosity silicon oil. The focusing was performed with a programmed run with rapid ramping steps until 1200 V and a slower phase until 8000 V, until a total of 47 kVh was reached.

After pouring off the oil, the focused strips were consecutively equilibrated for 15 min in 6 M urea, 30% glycerol [56-81-5], 3.3% Tris–HCl [1185-53-1] pH 8.8 and 2% SDS containing either 1% DTT (Buffer A) or 4% iodoacetamide [144-48-9] (Merck) (Buffer B) in the IEF running set-up. The strips were replaced on 1 mm thick 10% or 12% polyacrylamide [9003-05-8] (SDS–PAGE) gels (26 cm × 20 cm), embedded with 0.5% agarose [9012-36-6] supplemented with bromophenol blue [115-39-9] as a tracking dye. The proteins were separated with an electrode buffer system (0.01% SDS; 2.5 mM Tris–HCl, pH 8.3; 19.2 mM glycine [56-40-6]) according to Laemmli [35] at a constant current of 10 mA/gel and at 15 °C in the Ettan DALT 12 Separation Unit (Amersham Biosciences). The gels were silver-stained—slightly modified according to Blum [36]—digitally imaged using Fluor-S MultiImager (Bio-Rad) and analysed with PD-Quest Software 7.1.0 (Bio-Rad). The normalised quantity of optical density areas of the protein spots was calculated as the total quantity in valid spots and expressed as a percentage of the total volume in all spots present in the gel. The normalised values were exported to Excel 97 (Microsoft), averaged and analysed with the two-tailed Student's *t*-test ($p < 0.05$).

2.3. Identification of the protein spots

The spots of interest were cut out with shortened micropipette tips and automatically digested using a Tecan ProTeam DigestR instrument (Männedorf, Switzerland). In detail, protein containing gel plugs were dispensed into 96-well V-Bottom microtiter plates (V-Bottom, PP, Greiner) covered with a pierceable silicon mat in 50 μl wash buffer consisting of 50 mM ammonium bicarbonate [1066-33-7] (Merck) in 30% (v/v) acetonitrile [75-05-8] (VWR International).

Digestion was according to the following protocol: gel plugs were washed and equilibrated two times with each 50 μl, 50 mM ammonium bicarbonate in 30% (v/v) acetonitrile. Before addition of 2 μl trypsin [9002-07-7] (Roche) solution (12.5 ng/μl in 5 mM Tris–HCl, pH 8.0), the gel plugs were treated with 80% (v/v) acetonitrile to allow uptake of the aqueous trypsin solution.

Additional digest buffer (5 mM Tris–HCl, pH 8.0) was added to prevent evaporation during the digestion, which was allowed to proceed for 2 h at 37 °C in an enclosed and insulated on-deck incubator. After 2 h, the plate was robotically removed from the incubator and placed back on to the deck of the ProTeam DigestR instrument while the trypsin activity was terminated by addition of 12 μl 1% (v/v) trifluoroacetic acid [76-05-1] (VWR International). Peptides were purified robotically by an automated protocol utilising Millipore's ZipTipR technology, according to the manufacturer's recommendations. Purified peptides were eluted directly onto a Bruker's MALDI target plate (AnchorChipR 400-384) with 1.5 μl of a solution containing 90% (v/v) acetonitrile, 0.1% (v/v) trifluoroacetic acid plus 90 μg/ml alpha-hydroxycyanocinnamic acid (Bruker).

MALDI-MS analysis for protein identification was performed in a fully automated fashion on a Bruker Autoflex machine operated in reflector mode. Calibrated and annotated spectra were subjected to an automated database search utilising Bruker's BioTools 2.0 (Bruker) and the Mascot 1.7 search engine (Matrixscience).

2.4. Western blotting

Forty micrograms total protein of each extract was diluted with rehydration buffer and run on a 12% SDS–PAGE gel with a 5% stacking gel at a current of 15 mA/gel. Proteins were transferred to Hybond-P polyvinylidene fluoride (PVDF) [24937-79-9] (Amersham Biosciences) membrane. Membranes were blocked in PBST (PBS, 0.1% Tween20 [9005-64-5]) with 5% dry milk overnight. Membranes for hHSN3 analysis were probed with mouse monoclonal antibody to 20S proteasome subunit β7 (Biomol International) 1:700, for hPP-1A analysis with rabbit polyclonal antibody anti-protein phosphatase 1α, C-terminal (Calbiochem) 1:700 and for hUQCRC1 analysis with mouse monoclonal anti-OxPhos ComplexIII core 1 subunit (Molecular Probes) 1:700, all in AB Buffer (PBST with 1% bovine serum albumin). The blots were incubated with goat anti-rabbit or anti-mouse IgG alkaline phosphatase-linked secondary antibody (Amersham Biosciences) 1:2500 in AB Buffer and the bands were detected colorimetrically with Alkaline Phosphatase Conjugate Substrate Kit (Bio-Rad). Image analysis was done by Quantity One Software (Bio-Rad).

3. Results

To compare the nuclear proteome patterns of untreated TK6 cells with cells grown either in the presence of 1 μM As(III) or irradiated with 1-Gy ^{137}Cs-γ-rays or treated with both agents, three independent cell extract batches with the four differently treated samples were subjected to 2D-E, and replicate gels of each extract were run at least three times. After spot detection, background subtraction and volume normalisation, about 900–1400 spots were detected on the silver stained gels (Fig. 1a). The normalised spot intensities showing at least 1.6-fold difference as the mean value of the three cell extract batches compared with the control mean values in one or more of the exposure conditions were chosen for further identification with MALDI-TOF. Fig. 1b shows the segments of the 2D-gel map with the identified proteins with different treatments.

Of the 17 spots fulfilling the criteria mentioned above, it was possible to identify nine with high confidence. These proteins and their theoretical and observed p*I*- and M_r-values and the sequence coverage data are listed in Table 1. The observed p*I*- and M_r-values correlated well with the theoretical ones. However, in the case of electron-transfer flavoprotein subunit alpha a slight shift in the p*I*-value to the acidic side was observed, which may be due to a difference in the modification status of the protein. The highest sequence coverage (58%) was reached by proteasome subunit beta type 4 precursor with eleven matching peptides. The lowest score (27%) was measured for isocitrate dehydrogenase (NAD) subunit alpha with nine matched peptides.

Seven proteins showed significantly different values compared with control values ($p < 0.05$) in at least one of the exposure conditions. The relative spot volumes

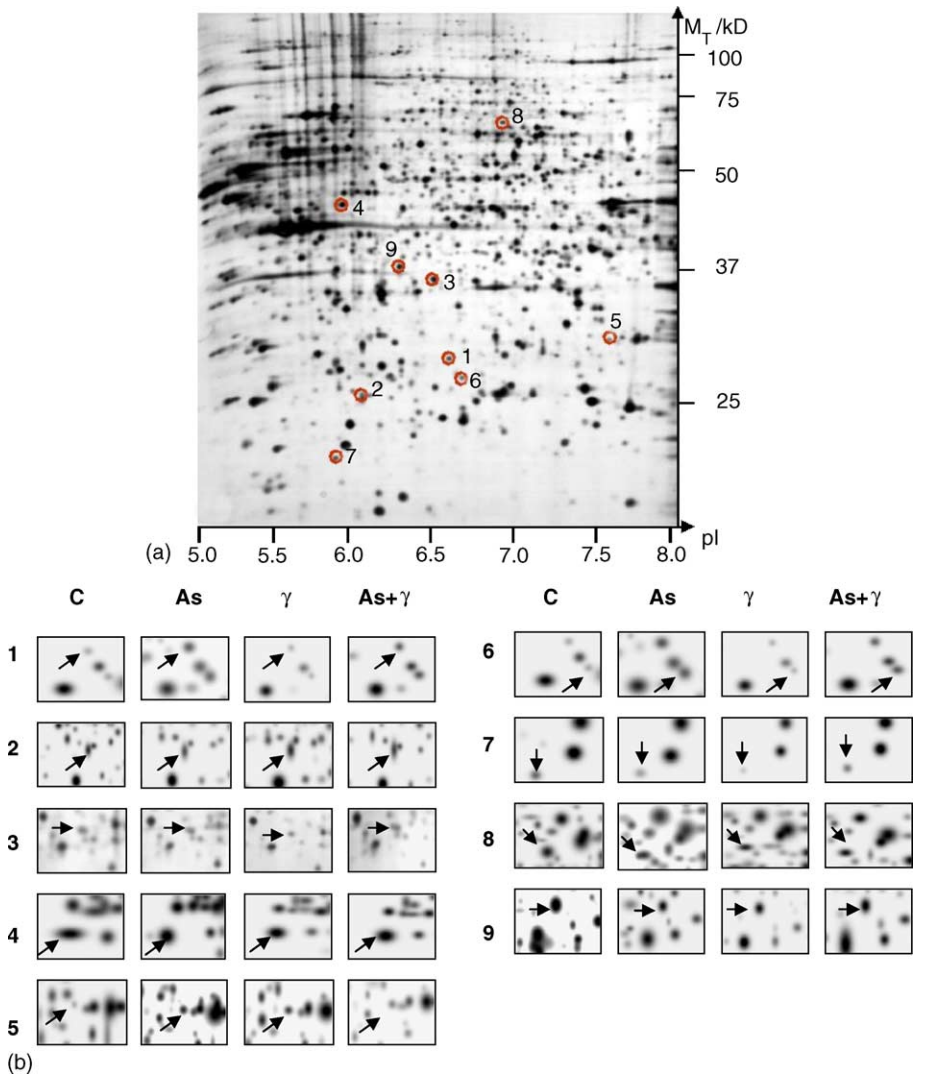

Fig. 1. (a) A representative gel image of the enriched core fraction of untreated TK6 cells visualised by two-dimensional gel (10%) and silver staining. Numbers refer to identified proteins (circled): (1) glutathione transferase omega 1; (2) proteasome subunit beta type 4 precursor; (3) serine/threonine protein phosphatase PP1-alpha 1; (4) ubiquinol-cytochrome *C* reductase complex core protein I; (5) electron transfer flavoprotein subunit alpha; (6) endoplasmic reticulum protein Erp29 precursor; (7) adenine phosphoribosyltransferase; (8) succinate dehydrogenase (ubiquinone) flavoprotein subunit; (9) isocitrate dehydrogenase (NAD) subunit alpha. (b) Segments of the 2D-gel map showing the identified protein spots (arrows) with different treatments. TK6 cells were either treated with 1 μM sodium arsenite (As) or irradiated with 1-Gy gamma (γ)-radiation or underwent both treatments (As + γ). The untreated cells are shown in the control lane (C). The numbers represent the same proteins as in Fig. 1a.

(%) and the standard deviations of these proteins are shown in Fig. 2. The protein functions, regulation factors and the statistical significance measured by the Student's *t*-test ($p < 0.05$) are shown in Table 2.

Two proteins, succinate dehydrogenase (ubiquinone) flavoprotein subunit (hDHSA) and isocitrate dehydrogenase (NAD) subunit alpha (hIDHA), both enzymes of the citric acid cycle, showed a clear

Table 1
Proteins identified in this study

SWISS-PROT accession no.	Abbreviation	Protein name	Theoretical pI/M_r	Experimental pI/M_r	Seq. Cov. %
P78417	hGSTO1-1	Glutathione transferase omega 1	6.24/27565.57	6.4/29000	43
P28070	hHSN3	Proteasome subunit beta type 4 precursor	5.72/29192.18	5.9/26000	58
P08129	hPP-1A	Serine/threonine protein phosphatase PP1-alpha 1	5.94/37512.08	6.4/37000	45
P31930	hUQCRC1	Ubiquinol-cytochrome *C* reductase complex core protein I	5.94/52618.79	5.8/49000	52
P13804	hETFA	Electron transfer flavoprotein subunit alpha	8.62/35097.57	7.5/31000	35
P30040	hERp29	Endoplasmic reticulum protein Erp29 precursor	6.77/28993.43	6.5/28000	34
P07741	hAPRT	Adenine phosphoribosyl transferase	5.79/19476.56	5.8/21000	57
P31040	hDHSA	Succinate dehydrogenase (ubiquinone) flavoprotein subunit	7.06/72691.51	6.8/66000	44
P50213	hIDHA	Isocitrate dehydrogenase (NAD) subunit alpha	6.46/39591.69	6.1/38000	27

tendency to decrease in all exposure conditions, but this difference did not reach statistical significance, possibly due to the large variation in the control values.

All identified proteins were also present in the cytosolic fraction but the exposed protein levels did not significantly differ from the control levels (data not shown). Assuming that the changes in the protein levels would be caused by protein trafficking between the cellular compartments, one would only see the differences in the nuclear fraction due to the much lower total protein concentration in the nucleus.

Three protein spots increased and four decreased significantly with at least one of the exposure conditions. Interestingly, in five cases the protein level corresponding to the combined exposure was not different from the control level, although differences were observed after the single exposures. For example, the amount of glutathione transferase omega 1

Table 2
The effect of As(III) and γ-radiation on protein amounts

Protein	Function	Regulation factor/p-values[a]				
		C vs. As	C vs. γ	C vs. As + γ	As vs. As + γ	γ vs. As + γ
hGSTO1-1	Glutathione metabolism, arsenic biotransformation	1.7↑/**0.0348**	1.4↓/0.1012	1.5↑/0.1086	1.2↓/0.2739	2.1↑/**0.0081**
hHSN3	Ubiquitin-dependent or -independent proteolyse	1.8↑/**0.0062**	2.1↑/**0.0002**	1.4↑/0.0956	1.3↓/0.0729	1.6↓/**0.0033**
hPP-1A	Cell division, apoptosis, glycogen metabolism	2.5↓/**0.0002**	2.9↓/**0.0001**	2.0↓/**0.0007**	1.3↑/0.1757	1.5↑/**0.0307**
hUQCRC1	Oxidative phosphorylation	2.0↓/**0.0420**	2.0↓/**0.0173**	1.6↓/0.0636	1.2↑/**0.0299**	1.2↑/0.2277
hETFA	Electron transfer to respiratory chain	1.9↑/**0.0092**	1.7↑/**0.0017**	1.8↑/**0.0027**	1.1↓/0.7955	1.1↑/0.6853
hERp29	Protein processing in ER	1.2↑/**0.2262**	2.5↓/**0.0083**	1.0/0.3059	1.2↓/0.1126	2.5↑/**0.0001**
hAPRT	Purine metabolism	1.4↓/**0.0136**	2.0↓/**0.0334**	1.2↓/0.0654	1.1↑/0.1440	1.6↑/0.0533

[a] The statistically significant p-values (<0.05) are printed bold.

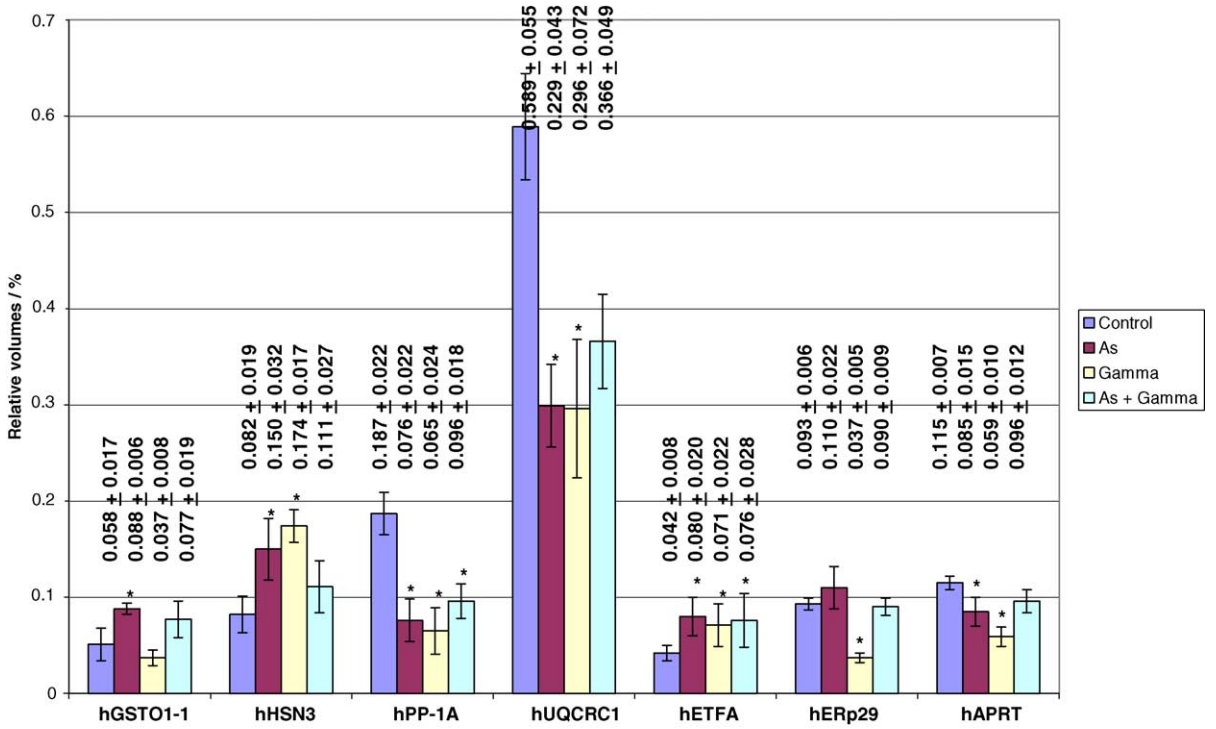

Fig. 2. The relative volumes (%) as a percentage of the total volume of all protein spots and the standard deviations of the identified proteins. The individual spot volumes are expressed as a percentage of the total volume in all spots present in the gel. Three independent cell extract batches with the four differently treated samples were subjected to 2D-E, and replicate gels of each extract were run at least three times. Significant differences between unexposed cells and cells exposed to arsenite, to radiation, or to both, based on a two-tailed Student's *t*-test ($p < 0.05$), are marked with an asterisk. hGSTO1-1, glutathione transferase omega 1; hHSN3, proteasome subunit beta type 4 precursor; hPP-1A, serine/threonine protein phosphatase PP1-alpha 1; hUQCRC1, ubiquinol-cytochrome *C* reductase complex core protein I; hEFTA, electron-transfer flavoprotein subunit alpha; hERp29, endoplasmic reticulum protein Erp29 precursor; hAPRT, adenine phosphoribosyltransferase.

(hGSTO1-1) increased only with arsenite, but not with the combined exposure. Similarly, the level of proteasome subunit β type 4 precursor (hHSN3) in the combined exposure was not different from the control level, although it showed a significant increase if exposed to arsenite or radiation. The intensity of electron-transfer flavoprotein subunit alpha (hETFA) increased under all exposure conditions.

Both ubiquinol-cytochrome *C* reductase complex core protein I (hUQCRC1) and adenine phosphoribosyl transferase (hAPRT) showed a significant decrease with arsenite or irradiation treatment only, but not when treated with both agents. The amount of endoplasmic reticulum protein ERp29 (hERp29) was significantly decreased only in the irradiation conditions. The amount of serine/threonine protein phosphatase PP1-α1 (hPP-1A) decreased significantly under all exposure conditions.

Two of the identified proteins (hUQCRC1, hETFA) are involved in the energy metabolism pathways such as the citric acid cycle and the respiratory chain (Table 2, Fig. 2). Two proteins are involved in protein processing (hERp29) and degradation (hHSN3), hGSTO1-1 in glutathione and arsenic metabolism and hAPRT in purine metabolism. hPP-1A is a phosphatase playing an important role in cellular signalling.

The aim was to confirm the results from the 2D analysis with Western blots. Unfortunately, only three antibodies, namely those for hHSN3, hPP-1A and hUQCRC1 were commercially available. The Western blot analysis for hHSN3 and hPP-1A showed a similar trend of induction or repression as seen with 2D-E

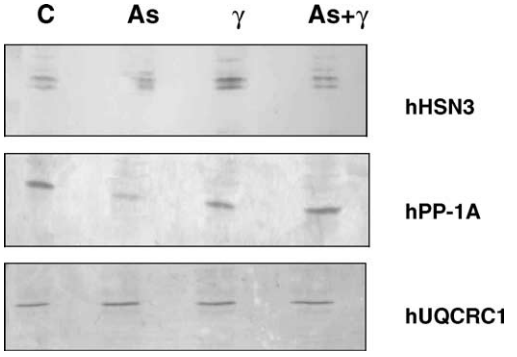

Fig. 3. Western blot analysis of three differentially expressed proteins with different treatments. TK6 cells were either treated with 1 μM sodium arsenite (As) or irradiated with 1-Gy gamma (γ)-radiation or underwent both treatments (As + γ) or were left untreated (C). The enriched nuclear proteins were subjected to Western blot analysis for the detection of three proteins (hHSN3, hPP-1A and hUQCRC1). The double band in hHSN3 represents the precursor (upper band) and the mature protein (lower band). The data are representative of at least three independent experiments.

(Fig. 3). However, in hPP-1A analysis, the cells treated with both arsenite and radiation had the same protein content as the control cells, and thus showed no decrease in the protein amount as in the 2D-E analysis. In the case of hUQCRC1, no significant differences in the protein amounts between the untreated and treated cells were found.

4. Discussion

By means of analysis of the whole nuclear proteome, it was possible to identify several proteins—some of them not yet known to be involved in the cellular metabolism—that were influenced by arsenite or γ-radiation.

It is shown for the first time that hGSTO1-1 is inducible by arsenite by a factor of 1.7 (Table 2, Fig. 2). Irradiation alone had no significant effect on the level of hGSTO1-1. Interestingly, irradiation of the cells treated with arsenite seemed to abolish the induction.

hGSTO1-1 is a member of the omega class of glutathione-*S*-transferases [37], identical to monomethylarsonic acid (MMA^V) reductase [38], the rate-limiting enzyme in inorganic arsenic metabolism. It catalyses the reduction of MMA^V to monomethylarsonous acid (MMA^{III}) with an absolute requirement for GSH [39]. Whereas GSH and most of the GST family members are involved in detoxification of ROS and other carcinogens [40] including arsenite [41], the formation of MMA^{III} by hGSTO1-1 is highly toxic; MMA^{III} is more cytotoxic and genotoxic and a more potent inhibitor of enzymes involved in the maintenance of the redox potential than arsenite in vitro and in vivo [42,43].

Many other members of the GST family [22] as well as GSH [44] are also induced by arsenite. The in vivo persistence of MMA^{III} which has been detected in the urine of humans drinking arsenic-contaminated water [45], and the putative correlation between polymorphisms in the gene for hGSTO1-1 and arsenic tolerance in humans [46] emphasize the importance of hGSTO1-1 in the cell and its inducibility by arsenite.

The induction of hGSTO1-1 may lead to accumulation of MMA^{III} and depletion of GSH. MMA^{III} is a potent inducer of apoptosis [47]. Previous data show that, in TK6 cells, 1 μM arsenite induces apoptosis significantly but at a low rate. In combination with 1-Gy γ-radiation arsenite has no additive effect on the rate of apoptosis and has a slight inhibitory effect on apoptosis with 2 Gy [31]. In addition, depletion of GSH is shown to induce apoptosis in some cell lines [48]. Therefore, the abolishment of the MMA^{III}-induced apoptosis could lead to an increased rate of transformation in the case of joint exposure.

The 2D-E method showed increased abundance of the β4 precursor of the 26*S* (20*S*) proteasome in the nuclear fraction by both arsenite or γ-radiation, whereas the cells exposed to both treatments showed no significant increase compared with the control level (Table 2, Fig. 2). Western blots showed an increase of both the precursor and the mature β4 protein, but only in the case of irradiated cells (Fig. 3). In agreement with our Western blot analysis, previous data show that the proteasome is a direct target for ionising radiation [49] whereas arsenite probably inhibits the ubiquitin conjugation step [50,51].

The 26*S* proteasome consists of a 19*S* regulatory subunit and a 20*S* core; the proteolytic activity is confined to the β-subunits of 20*S* [52]. 26*S* and 20*S* proteasomes are abundant and active in both cytosolic and nuclear compartments. Proteins are marked for degradation by covalent attachment to multiple molecules of ubiquitin and rapidly hydrolysed by the 26*S* proteasome in an ATP-dependent manner [53].

Under conditions of oxidative stress, the activity of nuclear 20*S* proteasomes rapidly increases [54] and the oxidised proteins are degraded by 20*S* without the requirement of ubiquitination or ATP hydrolysis. Nuclear degradation is important in non-lethal outcomes of cellular stress when proteins have to be down regulated rapidly in order to resume normal homeostasis [55].

It is interesting to note that the inhibition by arsenite of IR-induced p53 and p21 response observed by Vogt and Rossman [29] may be caused by the difference in degradation rates of the corresponding proteins between the single exposure (IR) and the combined exposure (IR and arsenite).

The fact that the degradation of key enzymes involved in apoptosis like transcription factor NF-κB [49], p53, p21, p27, retinoblastoma protein (pRb) and several cyclins [56] is controlled by the proteasome, makes it a possible modulator of many pro-oncogenical molecular changes. In cancer cells, which generally have higher levels of proteasome components and activity than their normal counterparts [57], the proteasome seems to inhibit apoptosis. Proteasome inhibitors activate apoptosis within hours; this process is supported by a simultaneous irradiation, several inhibitors being known as radiosensitisers. Proteasome inhibitors are currently tested in clinical trials as anticancer drugs.

In normal cell lines, proteasome plays a pro-apoptotic role early in the endogenous pathway [58]. We suggest that if arsenite is able to block the increase in proteasome activity induced by irradiation, as seen in the Fig. 3, the damaged cells may escape the normal apoptotic pathway and become more prone to transformation.

A general decrease in the amount of protein phophatase hPP-1A was observed for all exposure conditions in the 2D-E analysis (Table 2, Fig. 2) but only by arsenite if measured by Western blot analysis (Fig. 3). The differences between 2D-E and Western blot analysis may be due to several modification statuses of a protein, which on the 2D-E appear as several spots but on Western blots as a single band. The changes in the modification status are not the subject of this study and will need more clarification in the future. However, we definitely show the reduced expression of PP1α by arsenite. This is in agreement with previous data suggesting that arsenite inhibits several phosphatases [17,59,60], including serine/threonine phosphatases [61].

PP1 type enzymes regulate a variety of cellular processes such as cell division and meiosis, protein synthesis, glycogen metabolism, activation of receptors, ion channels and ion pumps [62]. In particular, PP1α plays a key role in the recovery from stress but promotes apoptosis when cells are damaged beyond repair [63]. PP1α is shown to directly dephosphorylate, and thus activate Bad, a pro-apoptotic member of the Bcl-2 family [64], subsequently, leading to caspase 3-dependent apoptose.

Protein phosphatases have been strongly linked to carcinogenesis in many studies [65]. Hyperphosphorylation of proteins due to phosphatase inhibition has been proposed for decades to be a general mechanism of carcinogenesis [66]. PP1α interferes with cell cycle control by dephosphorylating retinoblastoma protein (pRb) at the G1/S transition checkpoint [67]. Since the escape from G1 control is often considered a prerequisite for transformation, one may speculate that altered expression of PP1α has profound impacts on the proliferative potential and facilitates the ultimate transformation of a cell.

A quantitative change by arsenite and irradiation is seen in the levels of two enzymes involved in the mitochondrial respiratory chain (Table 2, Fig. 2). The level of ubiquinol-cytochrome *C* reductase complex core protein I (hUQCRC1), a part of the Complex III, is decreased by arsenite and irradiation separately, but we see no clear and significant effect by the joint exposure. The abundance of electron-transfer flavoprotein subunit alpha (hETFA), a protein delivering electrons to the respiratory chain, increases under all exposure conditions compared with the control.

In spite of the controversial outcome between the 2D-E and Western blot analyses (Fig. 3), our results give a hint of the involvement of mitochondria in the response to As and IR. It was unexpected to find a Complex III protein, normally embedded in the inner matrix of mitochondria, in the nuclear fraction. To study the mitochondrial proteins in further detail, a different type of cell fractionation procedure should be used. However, the interference by As and IR in the mitochondrial energy-linked functions has been well documented before [68,69] and the As-induced ROS formation occurs in the mitochondria [70].

A novel finding of this study is the involvement of the hERp29 precursor protein in the response to irradiation. The level of this protein is decreased 2.5-fold,

exclusively in the γ-irradiated cells (Table 2, Fig. 2). hERp29 was recently characterised as a novel reticuloplasmin localised in the ER lumen [71]. Reticuloplasmins participate in the early processing of proteins, i.e. folding, initial glycosylation and assembly of oligomers. hERp29 is expressed ubiquitously in mammalian tissues [72] and is encoded by a single gene highly conserved in mammalian evolution [73]. Although the exact function is not yet known, these and other attributes suggest that ER29 may play a unique and important role in the early protein processing.

Cells irreparably damaged by irradiation are forced to choose between apoptosis or transformation. Here, proteins that, firstly, inhibit apoptotic pathways or induce transformation pathways, and secondly, differ in the level of protein expression after combined exposure from that expected on the basis of the independent effect of single exposures are of special interest. It is concluded that the combined exposure to arsenite and radiation has significant antagonising effects on the abundance of proteins such as glutathione transferase omega, proteasome and serine/threonine phosphatase PP1-A, interfering with apoptotic or transformation pathways. A common feature of these and some other proteins found here is the involvement in the oxidative stress response and ROS formation. The co-carcinogenic effect of arsenic seen in vivo may partially be explained by the differential expression of these proteins. The proteomic screening method has proven to be a powerful tool in detecting novel protein candidates. Future research should focus on the elucidation of a more detailed mechanism of action and the role in the carcinogenic process of the proteins identified in this study.

Acknowledgements

We thank Frank Bunk, Markus Lang and Ernst Reich for excellent technical assistance and Dr. Guenther Stephan and Dr. Linda Walsh for critically reading the manuscript.

References

[1] H. Tinwell, S.C. Stephens, J. Ashby, Arsenite as the probable active species in the human carcinogenicity of arsenic: mouse micronucleus assays on Na and K arsenite, orpiment, and Fowler's solution, Environ. Health Perspect. 95 (1991) 205–210.

[2] W.P. Tseng, Effects and dose–response relationships of skin cancer and blackfoot disease with arsenic, Environ. Health Perspect. 19 (1977) 109–119.

[3] C. Hopenhayn-Rich, M.L. Biggs, A.H. Smith, Lung and kidney cancer mortality associated with arsenic in drinking water in Cordoba, Argentina, Int. J. Epidemiol. 27 (1998) 561–569.

[4] C.J. Chen, C.W. Chen, M.M. Wu, T.L. Kuo, Cancer potential in liver, lung, bladder and kidney due to ingested inorganic arsenic in drinking water, Br. J. Cancer 66 (1992) 888–892.

[5] P.R. Taylor, Y.L. Qiao, A. Schatzkin, S.X. Yao, J. Lubin, B.L. Mao, J.Y. Rao, M. McAdams, X.Z. Xuan, J.Y. Li, Relation of arsenic exposure to lung cancer among tin miners in Yunnan Province, China, Br. J. Ind. Med. 46 (1989) 881–886.

[6] L. Jarup, G. Pershagen, Arsenic exposure, smoking, and lung cancer in smelter workers–a case-control study, Am. J. Epidemiol. 134 (1991) 545–551.

[7] J.H. Lubin, L.M. Pottern, B.J. Stone, J.F. Fraumeni Jr., Respiratory cancer in a cohort of copper smelter workers: results from more than 50 years of follow-up, Am. J. Epidemiol. 151 (2000) 554–565.

[8] P.L. Goering, H.V. Aposhian, M.J. Mass, M. Cebrian, B.D. Beck, M.P. Waalkes, The enigma of arsenic carcinogenesis: role of metabolism, Toxicol. Sci. 49 (1999) 5–14.

[9] J.L. Yang, M.F. Chen, C.W. Wu, T.C. Lee, Posttreatment with sodium arsenite alters the mutational spectrum induced by ultraviolet light irradiation in Chinese hamster ovary cells, Environ. Mol. Mutagen. 20 (1992) 156–164.

[10] J.H. Li, T.G. Rossman, Mechanism of comutagenesis of sodium arsenite with *n*-methyl-*n*-nitrosourea, Biol. Trace Elem. Res. 21 (1989) 373–381.

[11] T.C. Lee, K.C. Lee, Y.J. Tzeng, R.Y. Huang, K.Y. Jan, Sodium arsenite potentiates the clastogenicity and mutagenicity of DNA crosslinking agents, Environ. Mutagen. 8 (1986) 119–128.

[12] J.K. Wiencke, J.W. Yager, Specificity of arsenite in potentiating cytogenetic damage induced by the DNA crosslinking agent diepoxybutane, Environ. Mol. Mutagen. 19 (1992) 195–200.

[13] T. Okui, Y. Fujiwara, Inhibition of human excision DNA repair by inorganic arsenic and the co-mutagenic effect in V79 Chinese hamster cells, Mutat. Res. 172 (1986) 69–76.

[14] P. Ramirez, L.M. Del Razo, M.C. Gutierrez-Ruiz, M.E. Gonsebatt, Arsenite induces DNA-protein crosslinks and cytokeratin expression in the WRL-68 human hepatic cell line, Carcinogenesis 21 (2000) 701–706.

[15] J.W. Yager, J.K. Wiencke, Inhibition of poly(ADP-ribose) polymerase by arsenite, Mutat. Res. 386 (1997) 345–351.

[16] K.A. Rein, B. Borrebaek, J. Bremer, Arsenite inhibits beta-oxidation in isolated rat liver mitochondria, Biochim. Biophys. Acta 574 (1979) 487–494.

[17] C.M. Schiller, B.A. Fowler, J.S. Woods, Effects of arsenic on pyruvate dehydrogenase activation, Environ. Health Perspect. 19 (1977) 205–207.

[18] F.X. Reichl, L. Szinicz, H. Kreppel, W. Forth, Effect of arsenic on cellular metabolism after single or repeated injection in guinea pigs, Arch. Toxicol. Suppl. 13 (1989) 363–365.

[19] A. Boveris, N. Oshino, B. Chance, The cellular production of hydrogen peroxide, Biochem. J. 128 (1972) 617–630.

[20] A. Barchowsky, L.R. Klei, E.J. Dudek, H.M. Swartz, P.E. James, Stimulation of reactive oxygen, but not reactive nitrogen species, in vascular endothelial cells exposed to low levels of arsenite, Free Radic. Biol. Med. 27 (1999) 1405–1412.
[21] S.X. Liu, M. Athar, I. Lippai, C. Waldren, T.K. Hei, Induction of oxyradicals by arsenic: implication for mechanism of genotoxicity, Proc. Natl. Acad. Sci. 98 (2001) 1643–1648.
[22] M. Schuliga, S. Chouchane, E.T. Snow, Upregulation of glutathione-related genes and enzyme activities in cultured human cells by sublethal concentrations of inorganic arsenic, Toxicol. Sci. 70 (2002) 183–192.
[23] P.P. Simeonova, M.I. Luster, Mechanisms of arsenic carcinogenicity: genetic or epigenetic mechanisms? J. Environ. Pathol. Toxicol. Oncol. 19 (2000) 281–286.
[24] S.M. Keyse, R.M. Tyrrell, Heme oxygenase is the major 32-kDa stress protein induced in human skin fibroblasts by UVA radiation, hydrogen peroxide, and sodium arsenite, Proc. Natl. Acad. Sci. 86 (1989) 99–103.
[25] M.R. Rossi, S. Somji, S.H. Garrett, M.A. Sens, J. Nath, D.A. Sens, Expression of hsp 27, hsp 60, hsc 70, and hsp 70 stress response genes in cultured human urothelial cells (UROtsa) exposed to lethal and sublethal concentrations of sodium arsenite, Environ. Health Perspect. 110 (2002) 1225–1232.
[26] T.S. Wang, C.F. Kuo, K.Y. Jan, H. Huang, Arsenite induces apoptosis in Chinese hamster ovary cells by generation of reactive oxygen species, J. Cell. Physiol. 169 (1996) 256–268.
[27] Y.C. Chen, S.Y. Lin-Shiau, J.K. Lin, Involvement of reactive oxygen species and caspase 3 activation in arsenite-induced apoptosis, J. Cell. Physiol. 177 (1998) 324–333.
[28] S. Takahashi, E. Takeda, Y. Kubota, R. Okayasu, Inhibition of repair of radiation-induced DNA double-strand breaks by nickel and arsenite, Radiat. Res. 154 (2000) 686–691.
[29] B.L. Vogt, T.G. Rossman, Effects of arsenite on p53, p21 and cyclin D expression in normal human fibroblasts – a possible mechanism for arsenite's comutagenicity, Mutat. Res. 478 (2001) 159–168.
[30] M. Tyers, M. Mann, From genomics to proteomics, Nature 422 (2003) 193–197.
[31] S. Hornhardt, M. Gomolka, R. Amannsberger, J. Semmer, S. Widemann, T. Jung, Comparative investigations of sodium arsenite, arsenic trioxide and cadmium sulfate in combination with gamma-radiation on apoptosis, micronuclei induction and DNA damage in a human lymphoblastoid cell line, in preparation.
[32] U.K. Chowdhury, B.K. Biswas, T.R. Chowdhury, G. Samanta, B.K. Mandal, G.C. Basu, C.R. Chanda, D. Lodh, K.C. Saha, S.K. Mukherjee, S. Roy, S. Kabir, Q. Quamruzzaman, D. Chakraborti, Groundwater arsenic contamination in Bangladesh and West Bengal, India, Environ. Health Perspect. 108 (2000) 393–397.
[33] J.L. Schwartz, R. Jordan, B.A. Sedita, M.J. Swenningson, J.P. Banath, P.L. Olive, Different sensitivity to cell killing and chromosome mutation induction by gamma rays in two human lymphoblastoid cell lines derived from a single donor: possible role of apoptosis, Mutagenesis 10 (1995) 227–233.
[34] A. Görg, C. Obermaier, G. Boguth, A. Harder, B. Scheibe, R. Wildgruber, W. Weiss, The current state of two-dimensional electrophoresis with immobilized pH gradients, Electrophoresis 21 (2000) 1037–1053.
[35] U.K. Laemmli, Cleavage of structural proteins during the assembly of the head of bacteriophage T4, Nature 227 (1970) 680–685.
[36] H. Blum, H. Beier, H.J. Cross, Improved silver staining of plant proteins, RNA and DNA in polyacrylamide gels, Electrophoresis 8 (1987) 93–99.
[37] P.G. Board, M. Coggan, G. Chelvanayagam, S. Easteal, L.S. Jermiin, G.K. Schulte, D.E. Danley, L.R. Hoth, M.C. Griffor, A.V. Kamath, M.H. Rosner, B.A. Chrunyk, D.E. Perregaux, C.A. Gabel, K.F. Geoghegan, J. Pandit, Identification, characterization, and crystal structure of the Omega class glutathione transferases, J. Biol. Chem. 275 (2000) 24798–24806.
[38] R.A. Zakharyan, A. Sampayo-Reyes, S.M. Healy, G. Tsaprailis, P.G. Board, D.C. Liebler, H.V. Aposhian, Human monomethylarsonic acid (MMA(V)) reductase is a member of the glutathione-*S*-transferase superfamily, Chem. Res. Toxicol. 14 (2001) 1051–1057.
[39] R.A. Zakharyan, H.V. Aposhian, Enzymatic reduction of arsenic compounds in mammalian systems: the rate-limiting enzyme of rabbit liver arsenic biotransformation is MMA(V) reductase, Chem. Res. Toxicol. 12 (1999) 1278–1283.
[40] S. Chouchane, E.T. Snow, In vitro effect of arsenical compounds on glutathione-related enzymes, Chem. Res. Toxicol. 14 (2001) 517–522.
[41] O. Ramos, L. Carrizales, L. Yanez, J. Mejia, L. Batres, D. Ortiz, F. Diaz-Barriga, Arsenic increased lipid peroxidation in rat tissues by a mechanism independent of glutathione levels, Environ. Health Perspect. 103 (Suppl. 1) (1995) 85–88.
[42] J.S. Petrick, F. Ayala-Fierro, W.R. Cullen, D.E. Carter, H. Vasken Aposhian, Monomethylarsonous acid (MMA(III)) is more toxic than arsenite in Chang human hepatocytes, Toxicol. Appl. Pharmacol. 163 (2000) 203–207.
[43] J.S. Petrick, B. Jagadish, E.A. Mash, H.V. Aposhian, Monomethylarsonous acid (MMA(III)) and arsenite: LD(50) in hamsters and in vitro inhibition of pyruvate dehydrogenase, Chem. Res. Toxicol. 14 (2001) 651–656.
[44] T.C. Lee, J.L. Ko, K.Y. Jan, Differential cytotoxicity of sodium arsenite in human fibroblasts and Chinese hamster ovary cells, Toxicology 56 (1989) 289–299.
[45] H.V. Aposhian, E.S. Gurzau, X.C. Le, A. Gurzau, S.M. Healy, X. Lu, M. Ma, L. Yip, R.A. Zakharyan, R.M. Maiorino, R.C. Dart, M.G. Tircus, D. Gonzalez-Ramirez, D.L. Morgan, D. Avram, M.M. Aposhian, Occurrence of monomethylarsonous acid in urine of humans exposed to inorganic arsenic, Chem. Res. Toxicol. 13 (2000) 693–697.
[46] L.L. Marnell, G.G. Garcia-Vargas, U.K. Chowdhury, R.A. Zakharyan, B. Walsh, M.D. Avram, M.J. Kopplin, M.E. Cebrian, E.K. Silbergeld, H.V. Aposhian, Polymorphisms in the human monomethylarsonic acid (MMA(V)) Reductase/hGSTO1 gene and changes in urinary arsenic profiles, Chem. Res. Toxicol. 16 (2003) 1507–1513.
[47] D.J. Thomas, M. Styblo, S. Lin, The cellular metabolism and systemic toxicity of arsenic, Toxicol. Appl. Pharmacol. 176 (2001) 127–144.

[48] K. Aoshiba, S. Yasui, K. Nishimura, A. Nagai, Thiol depletion induces apoptosis in cultured lung fibroblasts, Am. J. Respir. Cell. Mol. Biol. 21 (1999) 54–64.
[49] F. Pajonk, W.H. McBride, Ionizing radiation affects 26s proteasome function and associated molecular responses, even at low doses, Radiother. Oncol. 59 (2001) 203–212.
[50] N.S. Klemperer, C.M. Pickart, Arsenite inhibits two steps in the ubiquitin-dependent proteolytic pathway, J. Biol. Chem. 264 (1989) 19245–19252.
[51] D.S. Kirkpatrick, K.V. Dale, J.M. Catania, A.J. Gandolfi, Low-level arsenite causes accumulation of ubiquitinated proteins in rabbit renal cortical slices and HEK293 cells, Toxicol. Appl. Pharmacol. 186 (2003) 101–109.
[52] W.L. Gerards, F.W. Hop, I.L. Hendriks, H. Bloemendal, Cloning and expression of a human proteasome beta-subunit cDNA: a homologue of the yeast PRE4-subunit essential for peptidylglutamyl-peptide hydrolase activity, FEBS Lett. 346 (1994) 151–155.
[53] W. Heinemeyer, N. Trondle, G. Albrecht, D.H. Wolf, PRE5 and PRE6, the last missing genes encoding 20S proteasome subunits from yeast? Indication for a set of 14 different subunits in the eukaryotic proteasome core, Biochemistry 33 (1994) 12229–12237.
[54] O. Ullrich, T. Reinheckel, N. Sitte, R. Hass, T. Grune, K.J. Davies, Poly-ADP ribose polymerase activates nuclear proteasome to degrade oxidatively damaged histones, Proc. Natl. Acad. Sci. 96 (1999) 6223–6228.
[55] T.W. Joseph, A. Zaika, U.M. Moll, Nuclear and cytoplasmic degradation of endogenous p53 and HDM2 occurs during down-regulation of the p53 response after multiple types of DNA damage, FASEB J. 17 (2003) 1622–1630.
[56] M. Rolfe, M.I. Chiu, M. Pagano, The ubiquitin-mediated proteolytic pathway as a therapeutic area, J. Mol. Med. 75 (1997) 5–17.
[57] W.H. McBride, K.S. Iwamoto, R. Syljuasen, M. Pervan, F. Pajonk, The role of the ubiquitin/proteasome system in cellular responses to radiation, Oncogene 22 (2003) 5755–5773.
[58] L.M. Grimm, A.L. Goldberg, G.G. Poirier, L.M. Schwartz, B.A. Osborne, Proteasomes play an essential role in thymocyte apoptosis, EMBO J. 15 (1996) 3835–3844.
[59] M. Cavigelli, W.W. Li, A. Lin, B. Su, K. Yoshioka, M. Karin, The tumor promoter arsenite stimulates AP-1 activity by inhibiting a JNK phosphatase, EMBO J. 15 (1996) 6269–6279.
[60] K.J. Trouba, E.M. Wauson, R.L. Vorce, Sodium arsenite-induced dysregulation of proteins involved in proliferative signaling, Toxicol. Appl. Pharmacol. 164 (2000) 161–170.
[61] R.N. Huang, I.C. Ho, L.H. Yih, T.C. Lee, Sodium arsenite induces chromosome endoreduplication and inhibits protein phosphatase activity in human fibroblasts, Environ. Mol. Mutagen. 25 (1995) 188–196.
[62] H. Ceulemans, M. Bollen, Functional diversity of protein phosphatase-1, a cellular economizer and reset button, Physiol. Rev. 84 (2004) 1–39.
[63] A. Garcia, X. Cayla, J. Guergnon, F. Dessauge, V. Hospital, M.P. Rebollo, A. Fleischer, A. Rebollo, Serine/threonine protein phosphatases PP1 and PP2A are key players in apoptosis, Biochimie 85 (2003) 721–726.
[64] V. Ayllon, X. Cayla, A. Garcia, F. Roncal, R. Fernandez, J.P. Albar, C. Martinez, A. Rebollo, Bcl-2 targets protein phosphatase 1 alpha to Bad, J. Immunol. 166 (2001) 7345–7352.
[65] R. Parsons, Phosphatases and tumorigenesis, Curr. Opin. Oncol. 10 (1998) 88–91.
[66] H. Fujiki, Is the inhibition of protein phosphatase 1 and 2A activities a general mechanism of tumor promotion in human cancer development? Mol. Carcinog. 5 (1992) 91–94.
[67] C.W. Liu, R.H. Wang, M. Dohadwala, A.H. Schonthal, E. Villa-Moruzzi, N. Berndt, Inhibitory phosphorylation of PP1alpha catalytic subunit during the G(1)/S transition, J. Biol. Chem. 274 (1999) 29470–29475.
[68] H. Zhou, G. Randers-Pehrson, M. Suzuki, C.A. Waldren, T.K. Hei, Genotoxic damage in non-irradiated cells: contribution from the bystander effect, Radiat. Prot. Dosimetry 99 (2002) 227–232.
[69] N.A. Pham, D.W. Hedley, Respiratory chain-generated oxidative stress following treatment of leukemic blasts with DNA-damaging agents, Exp. Cell. Res. 264 (2001) 345–352.
[70] J. Pourahmad, P.J. O'Brien, F. Jokar, B. Daraei, Carcinogenic metal induced sites of reactive oxygen species formation in hepatocytes, Toxicol. In Vitro 17 (2003) 803–810.
[71] D.M. Ferrari, P. Nguyen Van, H.D. Kratzin, H.D. Soling, ERp28, a human endoplasmic-reticulum-lumenal protein, is a member of the protein disulfide isomerase family but lacks a CXXC thioredoxin-box motif, Eur. J. Biochem. 255 (1998) 570–579.
[72] E. Sargsyan, M. Baryshev, M. Backlund, A. Sharipo, S. Mkrtchian, Genomic organization and promoter characterization of the gene encoding a putative endoplasmic reticulum chaperone, ERp29, Gene 285 (2002) 127–139.
[73] M.J. Hubbard, N.J. McHugh, Human ERp29: isolation, primary structural characterisation and two-dimensional gel mapping, Electrophoresis 21 (2000) 3785–3796.